Nuclear Calibration of a Large Volume Calorimeter – 9318

S. Croft, S. Philips
Canberra Industries Inc.,
800 Research Parkway, Meriden, CT 06450, USA

E. Alvarez, K. Lambert,
2Canberra UK,
B528.10 Unit 1, Harwell Campus, Didcot, OX11 0TA, UK

J. Guerault,
Setaram Instrumentation
7 Rue de l'oratoire, 69300 CALUIRE, France

ABSTRACT

The non-destructive assay of canisters of Pu contaminated wastes and residues can be rendered impractical by traditional multiplicity counting techniques when the random to spontaneous fission neutron ratio is high since accidental coincidences swamp the signal. Provided a reliable isotopic vector for the principal heat-producing radio-nuclides can be obtained, with enough Pu present and sufficient measurement time, nuclear calorimetry offers a viable approach in many cases. Given the high precision and accuracy that can be typically obtained, calorimetry has long been an important tool for nuclear material accountability. More recently the technique has also been considered for bias-defect measurements as well as application to measuring minor actinides. The need for nuclear calorimetry to serve as the gold standard in the NDA of Pu (and certain other nuclear materials) has never been greater and yet expertise and commercial availability is declining. Here, we assess the performance of a commercially off the shelf (COTS) unit to gauge the current state of the practice.

In this work we report on the calibration of a COTS nuclear calorimeter of the twin cell design with an assay cavity of 15-liter capacity. The cavity is approximately 222mm x 292mm in cross section with a height of 272mm, originally being designed to accept glass blocks, but as such has the advantage that it can accept a diverse range of item shapes and sizes. Our focus has been to establish a calibration using a Joule effect heater and to compare it with a calibration performed using certified Pu reference material. We observed a modest heater cable effect and noted an apparent container specific baseline. We examined the impact of varying the spatial heat load pattern and performed some trials with mock 3013 storage containers. The results will be presented and discussed in terms of measurement accuracy as a function of power level.

INTRODUCTION

The thermal energy release by the radioactive decay of certain special nuclear materials can in many situations of practical importance be measured precisely and accurately against electrical or physical reference items. If the relative isotopic composition of the nuclear material is known the heat signature can be used to quantify the amount present. Nuclear calorimeters have a long history and have been used for nuclear materials accountancy to good effect throughout the fuel cycle [1]. A large variety of bespoke designs have been used over the past several decades to achieve particular measurement objectives. In this work we present results obtained with a simple general purpose 'room temperature' large volume, nearly isothermal, differential calorimeter, SETARAM Calo Series 270 [2]. The design is modular meaning that the measurement cell is readily scaleable in size [3]. The instrument used in this work had matching measurement and reference cells approximately 222mm x 292 mm x 272 mm (H) giving a nominal volume of about 18L suitable to accept a variety of container shapes and sizes. The heat flow between the container wall and the external wall is maintained at a fixed temperature by water circulating in a contoured pipe is determined from the differential signal between the array of Peltier coolers mounted in the symmetrical measurement and reference cells respectively.

Fig. 1. Photograph of the Calo Series 270 calorimeter used.

PU ITEMS AND THERMAL POWER ESTIMATES

The special nuclear material used in this work was a well characterized reactor grade PuO_2 in the form of a fine powder doubly encapsulated in welded stainless steel. A set of ten sources were available (nominally 0.1, 0.5, 1, 2, 5, 7, 10, 20, 25 and 25 g of Pu respectively) and all but the lowest mass items was used in the present work. Six power levels (17 to 460 mW) with a reasonable spacing were achieved by using combinations of the nine items. For the highest power level six items were combined while for the other

five power levels three items were used in each case so that the thermal mass remained about the same for the different combinations. The encapsulation system was the same for all of the sources and consisted of PuO_2 held firmly by a cup into the base of a inner capsule of 25mm internal diameter. The packing density of the powder is roughly 2 $g.mL^{-1}$. The inner capsule was welded shut before being placed into a snuggly fitting outer capsule of 30mm outer diameter which in turn had a lid welded into place. The external length of each assembly was approximately 58mm so that a stack of three could be fitted into the calorimeter when a rod-like heat source was needed to investigate spatial dependences. Otherwise the sources were measured as a cluster located close to the center of the measurement cell. To raise the sources so that the PuO_2 was roughly at the mid-plane of the cell a light-weight open-ended but inverted can (similar to a paint can or coffee can) was used.

In the context of this work the most important attribute of the sources is their thermal output, because the heat generated within them will eventually emerge irrespective of the details of their construction. The thermal power, P, expressed in units of mW, for the six source combinations is summarized in Table I. Measurements with Pu extended over the period 5th June 2008 to 26th June 2008 and the power quoted is the average of the power calculated for these two dates. The heat output at the end date was a factor 1.000433 times greater than at the start date. It is interesting to consider the fractional contribution of the various isotopes to the power. These are approximately 0.1173, 0.2899, 0.2992, 0.0057, 0.0002 and 0.2877 in the case of $^{238\text{-}242}$Pu and ^{241}Am respectively. Also given in Table I is the number of sources in each combination and the random uncertainty expressed as the relative standard deviation, rsd, in percent associated with weighing the mass of powder. This is based on combining in quadrature the estimated ±0.11mg (1-sigma) uncertainty in the net mass for each contributory source. In the context of other sources of uncertainty to be discussed later these are small uncertainties and so for practical purposes do not influence the analysis and conclusions. This is fortunate in that it means we can neglect the covariance between the combinations which arises because the combinations share sources.

Table I. Thermal power P (expressed in units of mW) for the six Pu source combinations (a-f). Power output is a mean value of values on 5th June 2008 and 16th June 2008. Also given is the number of source capsules per combination and the random weighing uncertainty expressed as a relative standard deviation in percent.

Combination	Number of source capsules	Power, P/mW	Random rsd/%
a	3	17.434	0.0048
b	3	52.298	0.0016
c	3	154.34	0.00054
d	3	248.95	0.00034
e	3	348.55	0.00024
f	6	460.61	0.00026

Far more important in determining the absolute uncertainty in the power outputs are the systematic uncertainties common to all of the source combinations. The uncertainty budget is given in Table II. The entries are quoted at the notional 68.26% confidence level (allowing for the number of degrees of freedom where finite observations have been made).

Table II. Systematic uncertainty budget for the nuclear heat output. Contributions are quoted in relative terms at the 68.26% confidence level (1-sigma for a normal distribution). The overall uncertainty listed is simply the quadrature sum of the individual relative standard deviations.

Contribution	rsd / %
Specific Powers	0.11
±1 day timing	0.0021
^{238}Pu half-life	0.0058
^{239}Pu half-life	0.000019
^{240}Pu half-life	0.000062
^{241}Pu half-life	0.034
^{242}Pu half-life	1.8×10^{-9}
^{241}Am half-life	0.00082
^{241}Pu β branching ratio	0.0000054
^{238}Pu abundance	0.15
^{239}Pu abundance	0.0086
^{240}Pu abundance	0.027
^{241}Pu abundance	0.027
^{242}Pu abundance	0.000047
^{241}Am abundance	0.0075
Pu/Oxide weight fraction	0.071
Balance Calibration	0.0003
Combined	0.20

In constructing Table II it should be noted that decay corrections for the isotopic composition since the date of the destructive analysis back in Jan 1990 have been made using half-lives and branching coefficients taken form the 1996 edition of the Table of Isotopes [4]. We made one exception and that was in the choice of the ^{241}Pu where we used a value of (14.33±0.03) *a* rather than (14.35±0.10) *a* based on our own review taking into account recent unpublished data. This reduces the uncertainty contribution a worthwhile amount. Specific powers for the individual isotopes were taken from ASTM C 1458-00 [5]. The individual contributions to the uncertainty were propagated and summed in quadrature to arrive at the term listed in Table II. A uncertainty of 1 day in the time between the isotopic determinations in 1990 and the date of measurement has been included. The 0.0021% impact reflects the increasing power that comes about by the in-growth of ^{241}Am. The uncertainties in the half-life and branching ratio affect the decay corrected composition and the uncertainties in the initial relative abundance impacts the mass of nuclides at the time of the heat measurements. An important

contribution comes from how well the weight fraction of Pu in the oxide was determined and a far less important contribution comes from the linearity of the analytical balance used to weigh the contents.

JOULE EFFECT

The thermal response of the calorimeter, $\mu V.mW^{-1}$ may be calibrated using an electrical heater made by winding a resistive wire around a metallic cylinder. The assembly is attached to a rectangular plate slightly smaller than the cross-section of the cells, and is fitted with short nylon legs. This arrangement ensures the heater is pretty much centered in the cavity. A dummy heater is placed in the reference cell although in the measurements reported here the dummy had no winding and nor did it have an electrical lead passing to the outside (Fig. 2). Standard practice is to electrically calibrate without a matrix (just air) although some trials were also done with a light weight aluminum foil matrix.

The desired electrical power dissipated as heat in the Joule effect heater is set in software and measured by the system controller. The accuracy of the controller is known through factory characterization measurements against measured powers determined using an accurately calibrated and precise voltmeter and an accurately calibrated and precise ammeter. In this work we take the power reading from the controller board. Over the power range 15 to 500mW we expect this to be a fair and unbiased estimate of the true power bounded by ±0.06%. The 1-sigma spot value is therefore likely to be less than this. Therefore, in the context of the present work the absolute uncertainty on the electrical power is superior to that which can be calculated from first principles for the Pu material by a factor of about 4, say.

Fig. 2. Photograph of the Joule effect heaters inside the calorimeter.

MOCK 2013 CONTAINERS

Engineered storage containers conforming to the US DOE 3013 prescription generally consist of an inner convenience can and two welded stainless steel cans. This can-in-can-in-can approach is expected to strongly influence the heat transfer dynamics (see for example the calculations by Santi et al [6] showing, in a different setting, the impact that the packing can exert) and was something we wanted to explore directly. Since our Pu source are already doubly encapsulated we dispensed with the convenience can and constructed a pair of mock 3013 inner and outer cans – one set for the measurement cell and one set for the reference cell.

The inner container was a cylinder 9" tall from base to open end, 4.5" OD with a wall thickness 0g 0.060". A cap made of the same material formed the lid. The lid had an indented spring loaded handled and attached loosely to the bottom piece by way of a pair of dog-legged slots which mated to a corresponding pair of spigots projecting from the perimeter near the rim. The outer container was of similar design but bigger. The open topped cylinder component was 10" long with a 0.375" thick base and lid. The wall thickness of the cylinder and cap was 0.125" with the OD of the bottom cylinder being 5". A similar handle and fastener were fitted. A schematic of the 3013 mock canister is given in Fig. 3 and a photograph is given in Fig. 4.

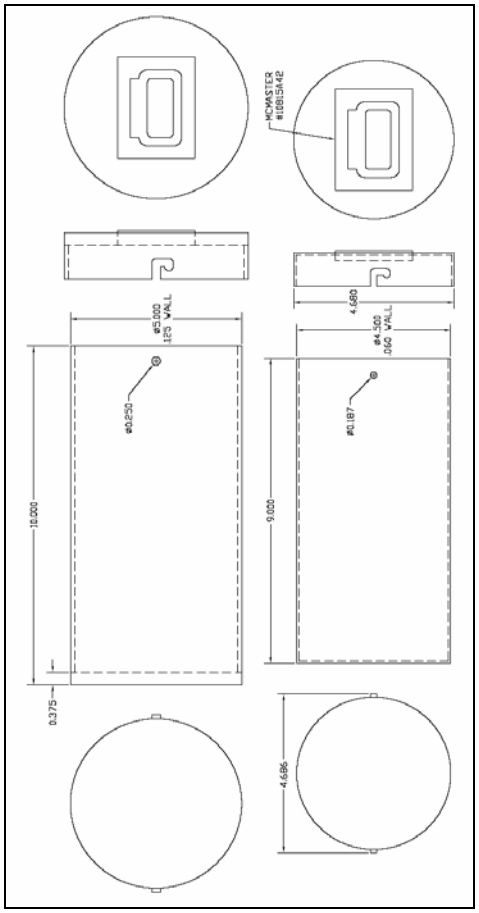

Fig. 3. Engineering sketch of the mock 3013 container used.

Fig. 4. Photograph of the mock 3013 container used.

DESCRIPTION OF EXPERIMENTS

The system was only available for a short period of time. The delivery boxes were left in the experimental area over the weekend. They were unpacked and the system components (computer, controller, chiller, assay chamber) interconnected in a period of about 2 hours on the Monday morning. A short settling period approximately 52 hours was allowed before the first run, an overnight acquisition with the electrical heater set to the upper range of interest, was begun. We began at the upper end so that residual fluctuations would be comparatively unimportant. The upper range was set by the Pu sources available rather than by a particular application. An advantage of the differential calorimeter design is that data collection can begin relatively quickly. The measurements extended from June 4th 2008 until June 27th. The chronological list of the different measurements taken with the Setaram calorimeter along with a brief description is provided in Table III in the annex. Some 35 runs were performed during this time. Local rules meant that the Pu items could not be measured during the night or at weekends. Therefore these periods were reserved for baseline (zero power) measurements and measurements of thermal power generated by the Joule Effect heater. The weekends afforded us the longest run times so that the stability of the baseline and plateaus at power could best be judged. Given the administrative burden of handling the Pu the daytime runs with the Pu items was typically limited to about 8 hours duration. The time to recover from the transient of opening the thermal shield to rearrange the contents and for the dynamics of the source to play out was therefore a significant part of the time available for observation. Ideally we would have liked to carry out some runs for considerably longer so that equilibrium could be established and monitored for long term stability. For instance we observed a tendency for the signal to overshoot very slightly (which we nonetheless compensated for and allowed for in the uncertainty budget) before settling which would have a small subtle influence on results formed from a simple mathematical end point prediction algorithm working on the rising curve.

No particular care was taken to control the environmental conditions in which the calorimeter sat. The measurements were carried out in a large radiation controlled area with tall thick concrete walls but a light overhead roof with windows running around the top which allowed sunlight to stream in at dawn and strike the assay system. The area was originally designed to be used as the target area of a van der Graaf accelerator. Industrial wall mounted heaters and coolers are installed but a large roller door to an outside compound remained in use during the measurement campaign. The temperature and humidity in the area was logged out of interest. Over a 24 h period the temperature could cycles a few ^{o}C in either direction about a nominal 19^{o}C. The Pu items were stored overnight in a safe which was cooler than the experimental room. The mock 3013 containers, Joule Effect Heater and its dummy companion were, however, simply kept beside the calorimeter until needed. In other words, in addition to not carefully controlling the temperature of the experimental area nor did we use any form of preconditioning (preheating) of the item under study. The benefit of doing so is probably marginal, however, when one considers the approach to equilibrium dominates over the initial transient phase. In the interests of minimizing the disruption to the assay cells and in the hope that it may serve to shorten the transient and reduce the comparative uncertainties we did tend to follow an electrical measurement by a Pu measurement of similar power.

Both the electrical and Pu calibrations comprised 7 power values (including the zero power baseline) and followed a similar spacing so that an almost one-to-one correspondence existed. In the event of any irregularities this would have provided a diagnostic check. In the event a linear fit was the most appropriate polynomial to both data sets. The upper power range investigated, about 450mW, was capped by the aggregate mass of Pu conveniently available. Our interest in a calorimeter of this design and size is primarily in assaying items of even higher power. Consequently we arbitrarily set a lower power cut off of about 15mW given we also wanted to include some repeat measurements as a matter of good practice and to tentatively check whether there was any dependence on the location of the heat source in the measurement cell. For this we arranged three source capsule on top of the other to form what we referred to as a Totem pole which we could place off axis.

Heat liberated within the measurement cell eventually must emerge through the faces and hence influence the embedded sensors. In this sense the signal at equilibrium is insensitive to the presence or mass of a benign matrix (i.e. one that is not undergoing a chemical or phase change for example). The rate of change of signal is matrix dependent though and in an effort to accelerate the initial transient we used Al foil, similar to baking foil in appearance, manually crumpled into low density objects roughly spherical in shape which we refer to as balls. It was hoped that the contact between the metallic balls would speed up and uniformly distribute the transport of heat from the items located in the measurement cell to the instrumented faces. The surfaces of the Al foil may be oxidized and also coated with an insulating layer of oil and so it was not obvious ahead of time that this scheme would improve matters. But because we felt it would do not harm and because there was the potential secondary benefit of reducing eddy current flow in the air

had we not used a filler we went ahead and included Al foil in some of the runs. Within the analytical power of these measurements we did not observe any significant difference in the quality of the assay result with or without foil. When the Pu capsules were placed inside the double walled mock 3013 containers the heat transport is certain to be strongly determined by the coupling of the capsules to the inner container and of the inner container to the outer container. The flow of heat through the base of the containers to the floor of the measurement cell is likely to be an important aspect. We only performed two runs with the Pu in the 3013 cans. We used the highest power to achieve the highest signal to noise ratio above the baseline. The baseline for the 3013 canisters seemed to be measurably different than for the Joule Effect heater and we therefore took disproportionately more baseline data in the case of the 3013's to make sure. The evolution of the signal for the 3013's was more gradual and so a larger projection was required to estimate the end point which also resulted is higher assigned uncertainties.

RESULTS

A complete summary of the numerical results may be found in the tables listed in the Annex. There are five categories of results. These are: Electrical Calibration with the Joule effect heaters; Pu Calibration in the mid-plane performed with the various combinations of sources; the spatial study made with the Totem poles; the 3013 Calibration; and the Inverted Pair measurements. The finding from each of these five studies will be commented on in subsequent sections.

An example of an electrical experiment is shown in Fig. 5. After the calorimeter is loaded there is a pronounced transient as the system responds to the severe thermal perturbation associated with having the lid opened and the measurement and reference items, which are at a different temperature to the interior, loaded . Given time the net signal will settle to a baseline value. The data acquisition is begun by the operator and is specified by setting a duration Z=(X+Y) and pulse width Y. The software waits for a period X=(Z-Y) for the system to settle before electrical power is applied for a period Y. An extra period X after the electrical pulse is added automatically to allow the system to return to the baseline again. However, since we had limited time quite often the runs were terminated early. In addition we tended to keep the settling period short so that baselines established in separate runs were averaged and recycled. In the case of electrical runs a sequence of power runs can be programmed, such as over the week end, allowing in our case two at power pulses to be sequenced.

In the case of the Pu measurements the calorimeter was loaded and the differential signal trace logged for as long a practical. The equilibrium value was estimated including allowance for empirical projection to the end point where necessary. The base line was estimated from runs where no heat source was present. The net signal (P) is the difference, $P=(P_E-P_B)$, between the equilibrium (P_E) and baseline (P_B) values and is given in units of μV.

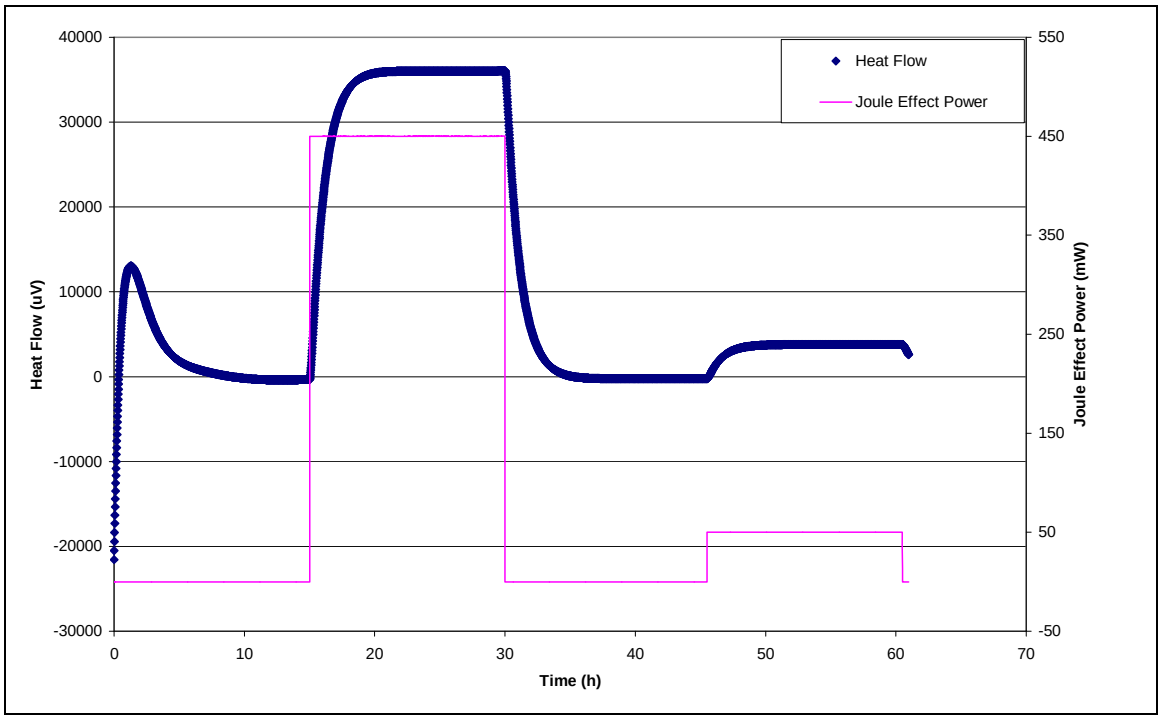

Fig. 5. Time trace of the response for an electrical calibration measurement.

Electrical Calibration

The set power was monitored by the controller and the random uncertainty was formed from the scatter in the data. It is much smaller that the systematic uncertainty assigned to the setting which was taken to be setting dependent. The uncertainty in the notional baselines corresponding to each of the runs which were performed on difference days an area subject to normal ambient variations is consistent with the root mean square (RMS) value of the at power uncertainty estimates. The uncertainty band assignments to the signal reflect the extrapolation uncertainty and is not merely a model uncertainty based on the assumption that a single exponential profile will correctly fit the data since a subjective contribution was factored in.

A weighted linear fit to the data, gave a slope of (80.592±0.21)μV.mW^{-1} with an intercept of (-234.97±32)mW with a covariance term of -4.203. Note repeat data was appropriately averaged before fitting. The ratio of the Fit to the Observed signal is consistent with unity within the combined uncertainty and above a power level of about 50mW the agreement is generally within about ±0.3%. This is consistent with the uncertainty in the slope from the fit of ±0.26%.

Pu Calibration

The uncertainty assigned to the Pu signals are a little larger than for the Joule effect measurements at the same nominal power since the extrapolation to equilibrium is somewhat longer owing to the shorter run lengths. In this case the systematic power level

is common to all points since it originates with the PuO_2 characterization. Thus in the fitting procedure only the random (weighing) contribution is included.

A weighted linear fit to the data, gave a slope of (80.793±0.059)μV.mW^{-1} with an intercept of (19.525±5.0)mW with a covariance term of -0.1036 between them. The ratio of the Fit to the Observed signal is again consistent with unity within the combined uncertainties and above a power level of about 50mW the agreement is within about ±0.4%. Note repeat data was appropriately averaged before fitting.

The intercept obtained for the Pu data is significantly different to that obtained with the Joule heaters. Sine the data collection was interleaved we don't think this was the result of the way the data collection was sequenced. Pending further investigation we suggest this may be a real effect associated with the fact that an electrical lead was only used to the powered heater and not to the dummy heater thereby creating a thermal comment from the measurement cell to the outside.

The ratio of the slope obtained from the Pu calibration to that obtained from the electrical calibration is equal to (80.793/80.592=) (1.0025±0.0034) where the quoted uncertainty includes the ±0.20% absolute uncertainty in the specific power level of the Pu items. This ratio is consistent with unity so that we conclude that, with the correct choice of baseline, the electrical and Pu calibrations match.

Inverted Tests

In principle we do not need to know the value of the baseline if measurements are performed in a matched pair closely spaced in time, by which we mean the item is measured twice once in the measurement cell and again in the reference cell. By reversing the roles of the roles of the two cells the signal is spread either side of the baseline so that only the spread matters. In our case the measurements were not concurrent but we can allow for a notional baseline stability. Pu and Joule data were collected at 461 and 450mW respectively and this allows the effective calibration constant to be extracted in this operating vicinity. The slope from the Joule data is (80.480±0.089))μW.mW^{-1} and from the Pu data (80.263±0.13) where the uncertainties are solely random. In forming the ratio we must also add the combined 0.21% uncertainty associated with the absolute knowledge of the electrical and Pu-thermal powers. The ratio of (0.9973±0.0029) is consistent with equivalency of the two calibrations – physical or electrical.

Totem Pole Analysis

At two power levels (350mW and 154mW) we have data taken with the sources taken in the mid-plane and also in the form of 'thermal rods' in two different places within the measurement cell. Because we have only a limited number of cases to compare the statistical power of the data is weak. However, the measurement results seem consistent in the 0.1% to 0.2% range arguing against any major spatial dependence. This is

supported also by the closeness of the Pu and Joule calibrations which have quite distinct heat distributions.

3013 Experiments

Following weighted averaging of the 461mW and zero power data the 3013 observations were analyzed analytically as a two point fit. The slope of (81.629±0.37)μV.mW-1 ,excluding systematic uncertainties, is a little higher than our other values but the uncertainty is also higher so we are consistent at the 2-3 sigma level. Given this is a single spot energy determination and for the 3013 container measured with less what are rather short durations we consider this agreement to be fair. It is encouraging that we are within 1% of the results obtained without the 3013 containment. Note the baseline for the 3013's is consistent with that observed for the other Pu experiments and again different to the Joule heater.

A plot of the two 3013 runs is given in Fig. 6. The initial transients and effective start times are different but that the trace begin to converge as the data collection proceeds. Run 19 has about 50 minutes extra observation time over run 25 meaning that the prediction to equilibrium is marginally less.

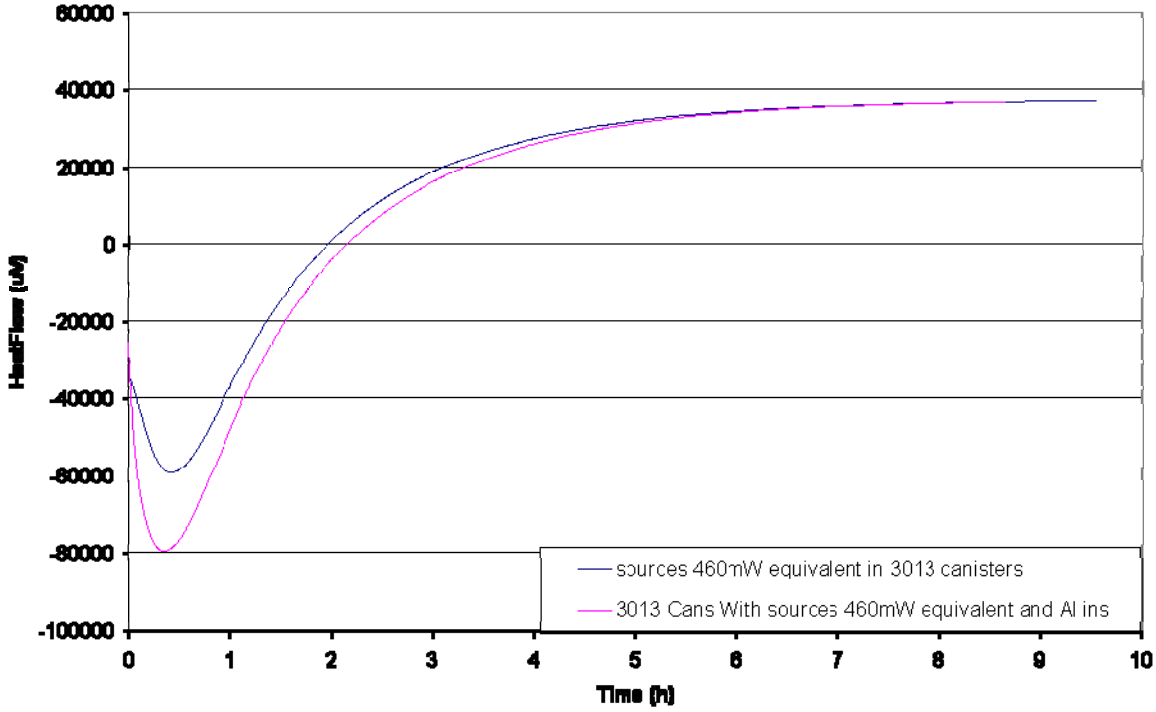

Fig. 6. Overlay of runs 19 and 25 for the 3013 container.

Discussion

Calorimetry can be used to measures the thermal power of nuclear items, most commonly as Pu and tritium, and in combination with knowledge of the relative isotopic composition of the contents provides a quantitative non-destructive estimate of the total Pu or tritium mass. Provided the long measurement time, compared to other NDA techniques such as quantitative gamma or combined gamma-correlated neutron, can be tolerated calorimetry can be a relatively simple and convenient approach capable of high accuracy. The convenience and accuracy stem from the fact that for suitably designed instruments the heat measurement is essentially independent of item geometry & packaging and independent of the spatial distribution of nuclear material (heat distribution) and also self-multiplication. At equilibrium the signal is independent of the matrix material & composition provided chemical reactions such as phase changes, curing, corrosion, rot and radiolysis are negligible. Furthermore electrical heat standards traceable to national standards are easy to construct and transport and may be used instead of Pu or tritium reference materials. The heat output of mixed oxide (MOX) nuclear fuel is insensitive to U and so calorimetry provides a direct assay of the Pu fraction. Baseline fluctuations depend on the environment in which the calorimeter is operated. Here differential or twin-compensation cell designs have two advantages - the first is the quicker settling period following set-up which come about by virtue of the signal being derived from the difference between two nominally matched cells; the second benefit is that the measurement room requires less careful control of the ambient conditions (in the present work we made no especial effort to control the temperature or humidity in the experimental hall and traffic to the outside continued). It is beneficial to include a dummy in the reference cell and as we have observed the dummy heater should have an electrical lead to math the thermal connection of the actual heater in the measurement cell. As we have seen in this work the thermal power may be determined to 0.1%. The accuracy of the assay may well then be limited by knowledge of the isotopic composition. For instance in the case of lean Pu residues or aged Pu the estimation of ^{241}Am content may be limiting. In the case of high burn-up Pu then the estimation of the ^{238}Pu content becomes limiting. Gold et al [7] provide a detailed account of how to evaluate uncertainties.

CONCLUSIONS

This paper summarizes a brief evaluation of a general purpose calorimeter. Electrical and nuclear calibrations were compared. The impact of heat location was tested. The effect of a 3013 style container on thermal dynamics was studied. The measurements were performed in an uncontrolled area and baseline fluctuations were found to be important. The assays were limited to about 8 hours durations and longer assays are needed to reach equilibrium. The importance of using a matched dummy in the reference cell, including electrical leads in the case of the Joule Effect heater is emphasized. The assay time is too long to carry out meaningful replicate measurements and so this work do not have the statistical power to assess uncertainties associated with heat source distribution., item weight, heater leads, controller stability, sensitivity to the environment including vibration and electrical power, operating procedure, end-point prediction etc.

ANNEX: SUMMARY OF EXPERIMENTAL RUNS AND NUMERICAL DATA

Table III. Chronological list of measurements taken with the Setaram calorimeter.

Run #	Description	Start time (all 2008)
1.	Joule Heating Cycle 450mW.	June 4th at 15:57.
2.	Source combination F on top of Al can (filled with 2m long strip of Al foil) sample cell filled with 15m of Al foil scrunched into balls. Reference cell contains can and foil as well. Thermal power ~461mW.	June 5th at 8:22.
3.	Joule heating Cycle 350 mW.	June 5th at 17:59.
4.	Source combination E on top of Al can (filled with 2m long strip of foil) sample cell filled with 15m of Al foil balls. Reference cell also contains a can and foil. Thermal power ~349mW.	June 6th at 8:12.
5.	and 6. Weekend measurement that comprises two Joule Heating Cycles: one at 450mW and the second one at 50mW.	June 6th at 16:06.
6.	Continuation of 5. Note, run 5/6 also provides a baseline estimate before and a baseline after the application of electrical power. The baseline before was a little too short and needed extrapolating. The one afterwards looks quite reasonable however.	
7.	Source combination B on top of Al can (filled with 2m foil) sample cell filled with 15m Al foil balls. Reference cell contains can and foil as well. Thermal power ~52mW.	June 9th at 8:28.
8.	Joule Heating Cycle 150 mW.	June 9th at 17:52.
9.	Source combination C on top of Al can (filled with 2m foil) sample cell filled with 15m Al foil balls. Reference cell contains can and foil as well. Thermal power ~154mW.	June 10th at 8:37.
10.	Joule Heating Cycle 50 mW.	June 10th at 17:22.
11.	Source combination D on top of Al can (filled with 2m foil) sample cell filled with 15m Al foil balls. Reference cell contains can and foil as well. Thermal power ~249mW.	June 11th at 8:34.
12.	Joule Heating Cycle 250 mW.	June 11th at 17:29.
13.	Repeat measurement of case number 2: Source combination F on top of Al can (filled with 2m foil) sample cell filled with 15m Al foil balls. Reference cell contains can and foil as well. Thermal power ~461mW.	June 12th at 8:34.
14.	Joule Heating Cycle 15 mW.	June 12th at 8:15.
15.	Sources combination A on top of Al can (filled with 2m foil) sample cell filled with 15m Al foil balls. The reference cell contains a support can and foil as well.	June 13th at 8:39.

	Thermal power ~17.4mW.	
16.	Weekend measurement with Al cans and foil but no sources. Thermal power is zero. This run is a good baseline for the Pu calibration.	June 13th at 17:14.
17.	Totem pole with source combination E surrounded in 4m of foil place on right front corner of the sample cell, cell filled with 15m foil. Similar setup in reference cell. Thermal power ~349mW.	June 16th at 8:50.
18.	3013 Canisters with 5 Al cans inside. Cells filled with foil. No sources. Thermal power is zero. One of several 3013 baseline runs.	June 16th at 17:58.
19.	3013 Canisters with 5 Al cans inside and source combination F on top of them. Cells filled with foil. Thermal power ~461mW. See also run 25.	June 17th at 8:46.
20.	Joule Heating elements inside measurement cells. No power was applied although it was supposed to come up to 450mW. The Reference and Sample cells had been switched around but inadvertently the electrically connections had not been flipped so that the thermal power was actually zero. This run should in principle serve as an additional baseline measurement but equilibrium was never achieved and so it was not used in the analysis.	June 17th at 18:34.
21.	Source combination F on top of Al can (filled with 2m foil) sample cell filled with 15m Al foil balls. Reference cell contains can and foil as well. The Reference and Sample cells were inverted as a check on symmetry of the differential system and so that we may use paired measurements to extract the power. Thermal power ~461mW.	June 18th at 8:54.
22.	Joule Heating Cycle 450mW. Reference and sample cells inverted to provide an electrical analog to match run number 21.	June 18th at 17:53.
23.	Totem pole with source combination E surrounded in 4m of foil place on right back corner of the sample cell, measurement cell was filled with 15m of Al foil. Similar setup in reference cell. Thermal power ~349mW.	June 19th at 8:44.
24.	3013 Canisters with 5 Al cans inside. Cells filled with foil. No sources. Zero thermal power.	June 19th at 17:41.
25.	3013 Canisters with 5 Al cans inside and source combination F on top of them. Cells filled with foil. Thermal power ~461mW. This is essentially a repeat of run 19 but the thermal perturbation of loading the items and the duration are of course different. The signal converges with that of run 19 rather nicely towards the end of the run but run 19 extends for about 50 minute	June 20th at 8:49.

	longer somewhat easing the projection to equilibrium.	
26.	3013 Canisters with 5 Al cans inside. Cells no foil. No sources. Zero power baseline run.	June 20th at 17:42.
27.	Totem pole with source combination C surrounded in 4m of foil place on right front corner of the sample cell, cell filled with 15m foil. Similar setup in reference cell. Thermal power ~154mW.	June 23rd at 8:59.
28.	Joule Heating Cycle 450mW, with foil filling the cells.	June 23rd at 17:50.
29.	Totem pole with source combination C surrounded in 4m of foil place on right back corner of the sample cell as viewed from the open lid, cell filled with 15m foil. Similar setup in reference cell. Thermal power ~154mW.	June 24th at 8:56.
30.	Baseline measurement, zero thermal power, with Al cans and foil but no Pu sources.	24th June at 8:56.
31.	Source combination B on top of Al can (filled with 2m foil) sample cell filled with 15m Al foil balls. Reference cell contains can and foil as well. This is a repeat measurement to case number 7. Thermal power ~52mW.	June 25th at 8:58.
32.	Baseline, zero power, with Joule Heaters in place, no Al foil.	25th June at 17:36.
33.	Source combination D on top of Al can (filled with 2m foil) sample cell filled with 15m Al foil balls. Reference cell contains can and foil as well. This is a repeat measurement to case number 11. Thermal power ~249mW.	June 26th at 8:56.
34.	3013 Canisters with 5 Al cans inside. Cells filled with foil. No sources. Thermal power is zero so this is another 3013 baseline measurement.	June 26th at 17:24.
35.	Baseline, thermal power of zero, with Joule Heaters in place and electrical cable connected, no Al foil. Reference and sample cells inverted (i.e. the heater is in the reference cell and the dummy is in the sample measurement cell) as a baseline check in the symmetrical arrangement corresponding to run 22. Equilibrium was not established and so this run was not used in subsequent analysis of the data.	June 27th at 15:11.

Table IV. Electrical Calibration data.

Run #	Power (mW)	Overall Unc.[a] (%)	Overall Unc. (mW)	Signal (μV)	Band (μV)	Base Line (μV)	Total (μV)	Fit (μV)	Unc. (μV)	Fit/Obs.	Unc.
1	450.13	0.08	0.36010	35930	24	24	33.9	36041.9	82.6	1.003115	0.002485
5	450.05	0.07	0.31504	36010	30	24	38.4	36035.5	81.3	1.000707	0.002498
28	449.86	0.08	0.35989	36175	30	24	38.4	36020.1	82.5	0.995719	0.002514

3	350.03	0.08	0.28002	27890	22	24	32.6	27974.6	62.3	1.003035	0.002521
12	249.88	0.08	0.19990	19940	28	24	36.9	19903.4	43.4	0.998162	0.002854
8	149.87	0.09	0.13488	11980	30	24	38.4	11843.4	29.4	0.988594	0.004007
6	49.99	0.08	0.03999	3796	10	24	26.0	3793.8	27.1	0.999427	0.009890
10	49.99	0.08	0.03999	3818	16	24	28.8	3793.8	27.1	0.993668	0.010331
14	14.98	0.07	0.01049	905	20	24	31.2	972.3	30.3	1.074363	0.049999
5	0	0	0	-237	12	0	12.0	-235.0	32.2	0.991435	0.144818
5	0	0	0	-290	80	0	80.0	-235.0	32.2	0.810241	0.249566
20	0							Not used			

[a] The 'overall uncertainty' is formed from the direct sum of the relative standard deviation (in %) and the bias (0.06% for all power measurements).

Table V. Pu Calibration data.

Run #	Power (mW)	Overall Unc.[a] (%)	Overall Unc. (mW)	Signal (μV)	Band (μV)	Base Line (μV)	Total (μV)	Fit (μV)	Unc. (μV)	Fit/Obs.	Unc.
2	460.61	0.00026	0.00119759	37335	50	30	58.3	37233.6	25.8	0.997284	0.001704
13	460.61	0.00026	0.00119759	37105	33	30	44.6	37233.6	25.8	1.003466	0.001393
4	348.55	0.00024	0.00083652	28190	35	30	46.1	28179.9	19.4	0.999643	0.001773
11	248.95	0.00034	0.00084643	20165	35	30	46.1	20132.9	13.8	0.998410	0.002382
33	248.95	0.00034	0.00084643	20045	40	30	50.0	20132.9	13.8	1.004387	0.002598
9	154.34	0.00054	0.00083344	12489	16	30	34.0	12489.1	8.7	1.000009	0.002810
7	52.298	0.0016	0.00083677	4292	30	30	42.4	4244.8	4.9	0.989011	0.009842
31	52.298	0.0016	0.00083677	4235	30	30	42.4	4244.8	4.9	1.002323	0.010107
15	17.434	0.0048	0.00083683	1459	15	30	33.5	1428.1	4.7	0.978801	0.022735
16	0	0	0	13	12	0	12.0	19.5	5.0	1.501923	1.438859
30	0	0	0	19	12	0	12.0	19.5	5.0	1.027632	0.700455

[a] The 'overall uncertainty' is the relative standard deviation (in %) with no bias added.

Table VI. Inverted tests data.

Run #	Power (mW)	Overall Unc.[a] (%)	Overall Unc. (mW)	Signal (μV)	Band (μV)	Base Line (μV)	Total (μV)
Pu:							
2, 13	460.61	0.00026	0.00119759	37190			111.0
21	460.61	0.00026	0.00119759	-36750	40	30	50.0
35	0	0	0	200	100	30	104.4
Joule:							
1, 5, 28	450.01	0.07	0.315007	36028			72.0
22	450	0.08	0.36	-36405	25	24	34.7

[a] The 'overall uncertainty' is formed from the direct sum of the relative standard deviation (in %) and the bias (0.06% for all electric calibration measurements and 0% for the Pu measurements).

Table VII. Totem Pole Analysis with Pu.

Run #	Power (mW)	Overall Unc.[a] (%)	Overall Unc. (mW)	Signal (μV)	Band (μV)	Base Line (μV)	Total (μV)
4	348.55			28190	35	24	42.4
17				28625	50	24	55.5
23				28568	30	24	38.4
Weighted by Total Uncertainty Mean:				28445			25.0[b]
							191.0[c]
							135.0[d]
9	154.34			12489	16	24	28.8
27				12725	25	24	34.7
29				12530	25	24	34.7
Weighted by Total Uncertainty Mean:				12569			19 [b]
							191 [c]
							135 [d]

[a] The 'overall uncertainty' is the relative standard deviation (in %) with no bias added.
[b] Internal Standard Error
[c] External Standard Deviation
[d] External Standard Error

Table VIII. 3013 experiments with Pu.

Run #	Power	Overall Unc.[a]	Overall Unc.	Signal	Band	Base Line	Total
	(mW)	(%)	(mW)	(μV)	(μV)	(μV)	(μV)
19	460.61	0.00026	0.00119759	37582	210	20	211.0
25	460.61	0.00026	0.00119759	37673	280	20	280.7
18	0			-52	60		
24	0			12	12		
26	0			20	10		
34	0			16	6		

[a] The 'overall uncertainty' is the relative standard deviation (in %) with no bias added.

REFERENCES

1. ANSI N15.22-1987, "American National Standard for nuclear materials – Plutonium-bearing solids calibration techniques for calorimetric assay", Publ. by ANSI, Inc., 1430 Broadway, New York, NY 10018.
2. J. GUERAULT, C. MATHONAT, G. ETHERINGTON, and S. CROFT, "Factory assessment of large volume nuclear calorimeters", Proc. 49th Annual meeting of the INMM (Institute of Nuclear Materials Management), July 13-17 2008, Nashville, Tennessee, USA. CD-ROM produced by Omnipress (2008).

3. C. MATHONAT and J-F. MAUGER, “Large volume and high sensitivity calorimetry for nuclear materials investigations”, Proceeding ESARDA (2007).
4. R.B. FIRESTONE, “Table of Isotopes Eighth Edition”, Volume II, John Wiley and Sons, Inc. (1996). ISBN 0-471-14917-9.
5. ASTM C 1458-00, “Standard test method for nondestructive assay of plutonium, tritium and ^{241}Am by calorimetric assay”, ASTM Book of ASTM Standards 2004, Section 12, Volume 12.01 Nuclear Energy (I) (2004)911-925, ISBN 0-8031-3756-7.
6. P.A. SANTI, D.S. BRACKEN, D.A. MACARTHUR and M.K. SMITH, “Use of fast calorimetry to perform mass attribute measurements”, Los Alamos National Laboratory Report LA-UR-07-3752 (2007), Presented at 48th Annual Meeting of the INMM, Tucson, AZ, USA, July 8-12, 2007.
7. A.S. GOLD, P. DE RIDDER and G. LASZLO, “Comparison between calorimeter and HLNCC errors”, 32nd Annual Meeting Proceedings, New Orleans, LA, USA July 28-31, 1991, Nuclear Materials Management XX(1991)767-770.